Enhanced purinoceptor-mediated Ca^{2+} signalling in L-fibroblasts overexpressing type 1 inositol 1,4,5-trisphosphate receptors

Richard J. DAVIS, R. A. John CHALLISS[1] and Stefan R. NAHORSKI

Department of Cell Physiology and Pharmacology, University of Leicester, Maurice Shock Medical Sciences Building, P.O. Box 138, University Road, Leicester LE1 9HN, U.K.

Mouse L-fibroblast cells stably transfected with either type 1 Ins(1,4,5)P_3 receptor (InsP_3R) cDNA (L15) or the vector control (Lvec) have been used to investigate the functional consequences of increased InsP_3R density on receptor-mediated Ca^{2+} signalling. L15 cells express approx. 8-fold higher levels of the type 1 InsP_3R compared with Lvec cells, which endogenously express essentially only the type 1 InsP_3R protein. Stimulation of Lvec and L15 cells with UTP or ATP increased cytosolic Ca^{2+} concentration to a greater extent in L15 cells at all agonist concentrations. UTP and ATP were equipotent, suggestive of the presence of endogenous cell-surface metabotropic $P2Y_2$-purinoceptors. In both cell clones the purinoceptors were coupled via pertussis-toxin-insensitive G-protein(s) to phospholipase C activation, resulting in similar concentration-dependent accumulations of InsP_3. Single-cell microfluorimetry revealed that overexpression of InsP_3Rs reduced the threshold for purinoceptor-mediated Ca^{2+} signalling. L-fibroblasts also exhibited temporally complex sinusoidal cytosolic Ca^{2+} oscillations in response to submaximal agonist concentrations, with significant increases in oscillatory frequencies exhibited by cells overexpressing InsP_3Rs. Sustainable oscillatory responses were dependent on Ca^{2+} entry and, at higher agonist concentrations, cytosolic Ca^{2+} oscillations were superseded by biphasic peak-and-plateau Ca^{2+} responses. Overexpression of InsP_3Rs in L15 cells resulted in a 4-fold reduction in the threshold for this change in the temporal pattern of Ca^{2+} mobilization. These data provide the first direct evidence demonstrating that altering the expression of the type 1 InsP_3R significantly affects receptor-mediated InsP_3-induced Ca^{2+} mobilization.

Key words: recombinant InsP_3 receptor expression, sinusoidal Ca^{2+} oscillations, UTP.

INTRODUCTION

Agonist activation of many G-protein-coupled receptors results in activation of phosphoinositide-specific phospholipase C and formation of Ins(1,4,5)P_3 (InsP_3) [1]. This second messenger mobilizes intracellular Ca^{2+} by interacting with its own tetrameric ligand-gated Ca^{2+}-release channel that can comprise one or more of the three receptor isoforms of InsP_3R that are encoded by distinct genes in mammals [2–5]. Despite sharing considerable homology in terms of amino acid sequence and domain layout, each isoform can exhibit differing binding affinities for InsP_3, tissue distributions, expression levels, and potential regulation by cytosolic Ca^{2+}, InsP_3 itself and phosphorylation by protein kinases [6–12].

Further complications may arise, since both homo- and hetero-tetramers of different isoforms are found in cells [11], and changes in InsP_3R expression could play a crucial role in the overall responsiveness of cells to agonists that act on receptors linked to the phosphoinositide cascade. Indeed, there is now substantial evidence that chronic activation of such cell-surface receptors can lead to a marked down-regulation of types 1 and 3 InsP_3Rs [13–15], and a consequent reduction in the ability of InsP_3 to mobilize Ca^{2+}. It has also been suggested that this could represent a mechanism of heterologous desensitization for Ca^{2+}-mobilizing agonists [13,15]. Furthermore, there is evidence that type 1 InsP_3R is progressively increased by retinoic acid-induced cellular differentiation of HL-60 cells [16], and a dramatic elevation of type 3 InsP_3Rs appears to accompany apoptosis in B- and T-lymphocytes [17]. However, the functional consequences of such altered expression are complicated by potential changes to other components of signal-transduction cascades induced by such manipulations.

In an attempt to gain a greater insight into the consequences of altered expression of InsP_3Rs, we have examined agonist-mediated phosphoinositide and Ca^{2+} signalling in a mouse L-fibroblast cell line that has been reported to endogenously express essentially only the type 1 InsP_3R [18]. This cell line has been transfected with type 1 InsP_3R cDNA (L15) and it stably expresses $\approx$ 8-fold greater levels of this receptor compared with the control cell line transfected with vector alone (Lvec) [18,19]. Here we utilize an endogenous purinoceptor in L-cells [20] to stimulate phosphoinositide hydrolysis and reveal significant changes in agonist-mediated Ca^{2+} signalling that accompanies altered InsP_3R expression.

MATERIALS AND METHODS

Cell culture

L15 cells, a stably transfected mouse L-fibroblast cell-line over-expressing the type 1 InsP_3 receptor protein, and Lvec cells (the vector-control cell-line), initially a gift from Professor K. Mikoshiba (Department of Molecular Neurobiology, Institute of Medical Sciences, University of Tokyo, Tokyo, Japan), were used between the first and fifteenth passages. The cells were

Abbreviations used: InsP_3, Ins(1,4,5)P_3; InsP_3R, type 1 InsP_3 receptor; KHB, Krebs–Henseleit buffer; $[Ca^{2+}]_i$, intracellular Ca^{2+} concentration; $[Ca^{2+}]_e$, extracellular Ca^{2+} concentration; PTX, pertussis toxin; Tg, thapsigargin; SERCA, sarco-/endo-plasmic-reticular Ca^{2+}-ATPase; fura-2/AM, fura-2 acetoxymethyl ester; 2MeS-ATP, 2-methylthio-ATP.

[1] To whom correspondence should be addressed (e-mail jc36@le.ac.uk).

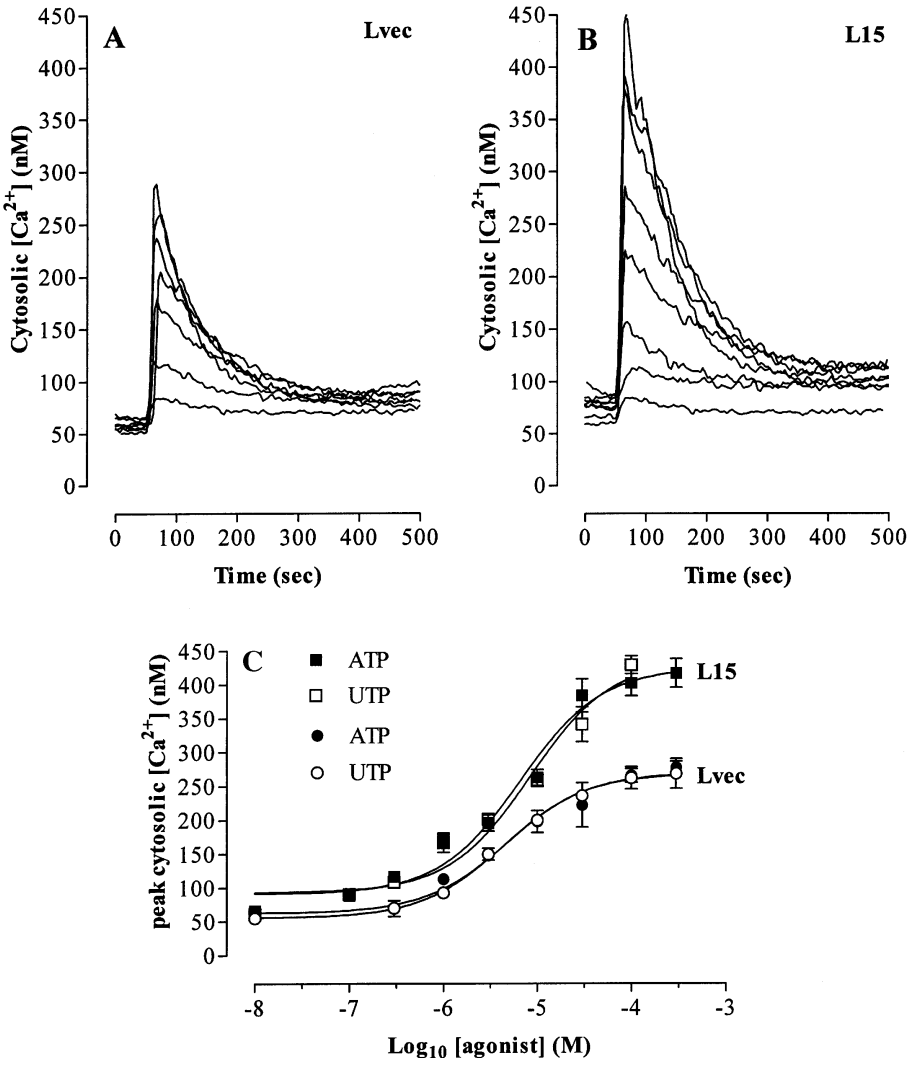

Figure 1 Effects of InsP_3R overexpression on purinoceptor-mediated increases in cytosolic Ca^{2+} concentration in suspensions of Lvec and L15 cells

Addition of increasing concentrations of UTP (0.1–300 μM) to fura-2-loaded (2 μM, 60 min) Lvec (**A**) and L15 (**B**) cell populations, caused biphasic peak and plateau Ca^{2+} responses at all agonist concentrations. Time-course traces are representative of a single response at each concentration, from three to eight identical experiments. (**C**) Peak Ca^{2+} increases at all UTP and ATP concentrations were significantly greater in L15 than in Lvec cells ($P < 0.01$, two-way analysis of variance). Data are shown as means ± S.E.M. from three to eight separate experiments at each concentration.

cultured in 175 cm^2 flasks, at 37 °C, in a 5 %-CO_2 incubator in Dulbecco's minimal essential medium (containing Hepes, sodium pyruvate and D-glucose), supplemented with 10 % (v/v) fetal-calf serum, 2 mM glutamine, 50 i.u./ml penicillin and 50 μg/ml streptomycin. Medium was replaced every 48 h, and cells sub-cultured (approx. every 7 days) by trypsin treatment on reaching confluency. For single-cell microfluorimetry and immunocyto-chemistry, cells were grown to 5–20 % confluency on 22-mm-diameter, 1.5-mm-thick, glass coverslips (Chance-Propper Ltd., Warley, West Midlands, U.K.), for 16–20 h prior to use, and maintained under the previously described conditions. For measurements of InsP_3 mass accumulation, cells were grown to confluency in 24-well multidishes.

Immunocytochemical analysis

Coverslips of Lvec and L15 cells were washed with PBS (2 × 10 min) at 22 °C. Fixation was achieved using 4 % (w/v) para-formaldehyde for 3 min, followed by three further washes with PBS. Fixed cells were permeabilized by treatment with 0.1 % Triton X-100 in 10 % goat serum/PBS for 30 min, followed by further washing. Permeabilized cells were incubated with a type 1 InsP_3R primary antibody (CT-1) at a dilution of 1:1000 in 10 % goat serum/PBS for 120 min followed by further washes with PBS, and FITC-conjugated anti-rabbit IgG (1:250) was then added for 60 min, followed by three further PBS washes. Excess fluid was carefully removed and the coverslip mounted using Citifluor-AF1 (UKC, Canterbury, Kent, U.K.). Coverslips were viewed at 500 × magnification using a laser scanning confocal microscope (Bio-Rad Lasersharp MRC-600). All measurements were taken using the same machine settings to allow direct comparisons to be made between the two cell lines.

Measurements of InsP_3 mass accumulation

Cells grown in 24-well multidishes were washed twice with Krebs–Henseleit buffer (KHB; in mM: NaCl, 118; KCl, 4.7; $NaHCO_3$, 4.2; $MgSO_4$, 1.2; KH_2PO_4, 1.2; $CaCl_2$, 1.8; glucose,

11.7; Hepes, 10; pH 7.4) and incubated at 37 °C for 30 min prior to agonist challenge. Reactions were terminated by the addition of 0.5 M ice-cold trichloroacetic acid. InsP_3-containing extracts were neutralized by the addition of 1:1 (v/v) tri-n-octylamine/1,1,2-trichlorotrifluoroethane and assays were performed using an InsP_3-binding protein as previously described [21].

Measurement of $[Ca^{2+}]_i$ in populations of cells

L15 and Lvec cells, 1 day post-confluent, were harvested from a 175 cm^2 flask ($\approx 5 \times 10^6$ cells) by agitation, using Hepes-buffered saline/EDTA (0.02% EDTA/0.9% NaCl/10 mM Hepes, pH 7.2) and then centrifuged at 500 ***g*** for 2 min. Cells were washed twice with KHB, and resuspended in KHB at an approximate density of 1×10^6 cells/ml. Cells were incubated with 2 μM fura-2 acetoxymethyl ester (fura-2/AM; Calbiochem) for 60 min at room temperature. Alternate 340 nm and 380 nm excitation wavelengths and 509 nm emission wavelength fluorescence measurements were made using a Perkin–Elmer LS50 luminescence spectrophotometer. The R_{max} and R_{min} values were determined at the end of each experiment by the addition of 0.1% Triton X-100 and 10 mM EGTA respectively (R_{max} is the 340/380 nm ratio obtained at saturating $[Ca^{2+}]$; R_{min} is the 340/380 nm ratio obtained at zero $[Ca^{2+}]$). Determination of the R_{max} with the Ca^{2+} ionophore ionomycin gave equivalent values. Cell autofluorescence was determined in parallel experiments and subtracted. Intracellular $[Ca^{2+}]$ estimates were derived from the ratio of emission intensities for 340/380 nm excitation using the Grynkiewicz equation [22]:

$$[Ca^{2+}]\ (nM) = K_d[(R - R_{min})/(R_{max} - R)] \times [(Sf_{min})/(Sf_{max})]$$

in which K_d is the dissociation constant for Ca^{2+}–fura-2 binding (135 nM at 22 °C), R is the observed 340/380 nm ratio, and Sf_{min}/Sf_{max} is the fluorescence ratio of $Ca^{2+}{}_{bound}/Ca^{2+}{}_{free}$, excited at a wavelength of 380 nm.

Single-cell Ca^{2+} imaging

Culture medium was replaced with KHB and cells were dye-loaded by incubation with 2 μM fura 2/AM for 60 min at room temperature. Coverslips were washed twice with KHB and then mounted on the stage of a Nikon–Diaphot inverted epi-fluorescence microscope ($\times 40$ objective). A field of 10–15 cells was selected and perfused with KHB at a rate of 5 ml/min for $\geqslant$ 10 min, prior to the start of the experiment. Experiments in the absence of extracellular Ca^{2+} were conducted in nominally Ca^{2+}-free KHB ($\leqslant$ 2 μM), which was perfused over cells for $>$ 10 min before the start of the experiment. Agonist addition was by continual perfusion at a rate of 5 ml/min. Fluorescent images were obtained by alternate excitation at 340 nm and 380 nm using an xenon arc lamp, with four consecutive images averaged over 1600 ms. The emission signal at 510 nm was measured using an intensified charge-coupled-device camera (Photonic Science, Robertsbridge, East Sussex, U.K.), with background fluorescence subtracted. Ratiometric values were converted into $[Ca^{2+}]_i$ using a calibration curve determined from the fluorescence of fura-2 free acid under saturating and chelating conditions, and the previous equation [22]. Single-cell measurements were obtained using Quanticell 700 software (Applied Imaging, Sunderland, Tyne and Wear, U.K.). Graphical interpretation of data was performed using Version 2.1 of GraphPad Prism (GraphPad Software, San Diego, CA, U.S.A.).

RESULTS

In confirmation of previous studies [18,19], increased expression of the type 1 InsP_3R in L15 compared with Lvec cells was clearly discernible using either radioligand binding methods (results not shown) or by immunocytochemical detection and laser scanning confocal microscopy (see Figure 4A below).

Endogenous P2Y purinoceptors mobilize Ca^{2+} from intracellular stores in Lvec and L15 cells

Purinoceptor activation by ATP or UTP (0.1–300 μM) in fura-2-loaded L15- and Lvec-cell populations caused rapid ($<$ 10 s) concentration-dependent transient peak elevations of cytosolic $[Ca^{2+}]$, followed by a lower plateau phase (Figures 1A and 1B). Resting cytosolic $[Ca^{2+}]$ in unstimulated cells was significantly higher in L15 cells compared with Lvec cells (75 $\pm$ 9 versus 50 $\pm$ 4 nM respectively; $n = 5$; $P < 0.05$). Peak and plateau Ca^{2+}

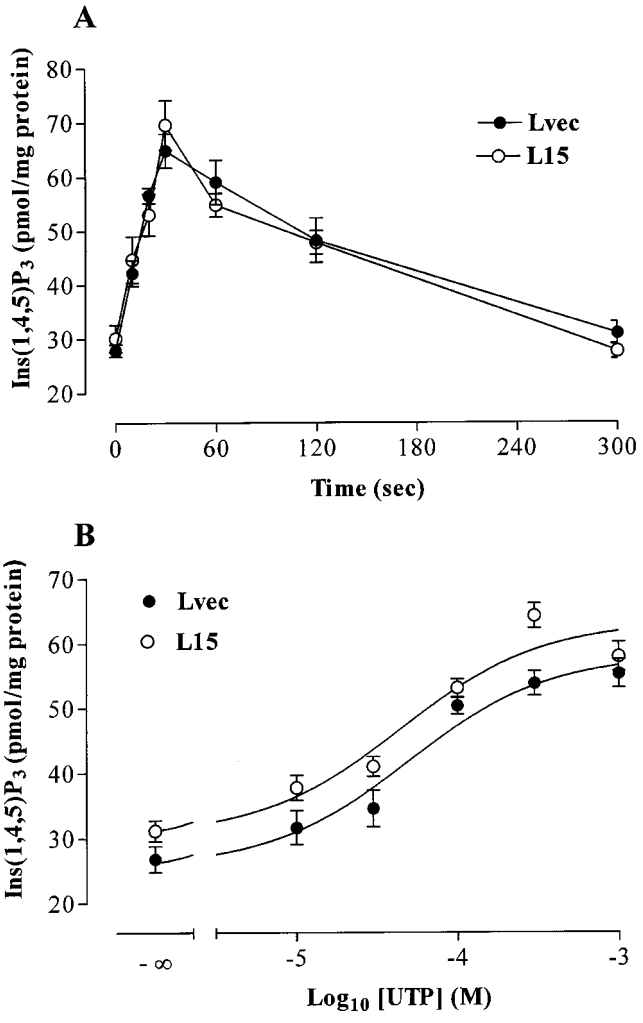

Figure 2 Time-course and concentration–response relationships for UTP-stimulated InsP_3 accumulation in Lvec and L15 cells

(**A**) Lvec and L15 cells exhibited similar time courses of InsP_3 accumulation in response to a maximally effective concentration of UTP (300 μM). (**B**) InsP_3 accumulation was also assessed in Lvec and L15 cells in response to a 30 s exposure to UTP (10–1000 μM). Data are shown as means $\pm$ S.E.M. for three to five separate experiments performed in duplicate.

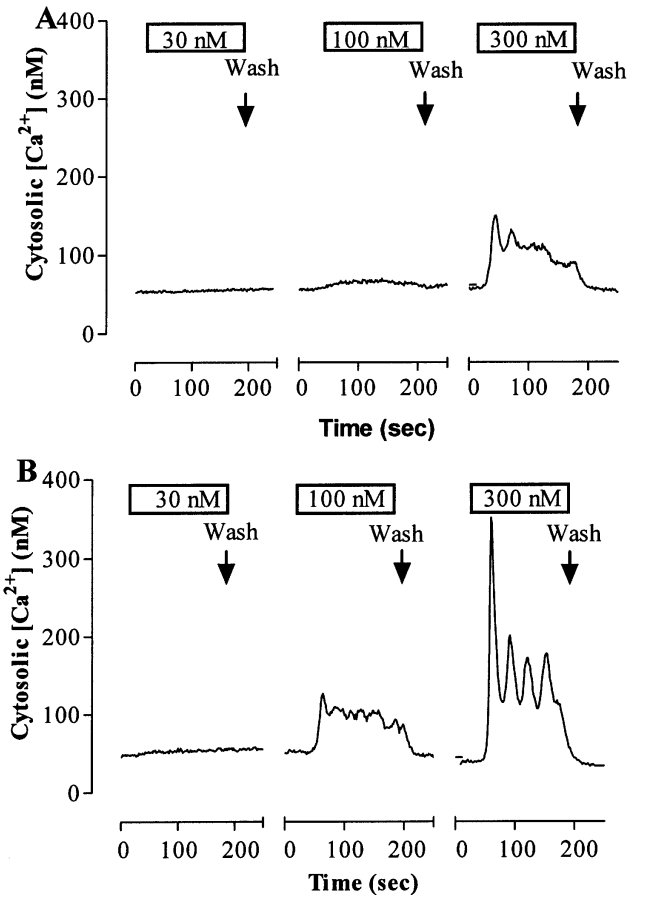

Figure 3 Effect of InsP_3R overexpression on the threshold concentration of agonist required to evoke a Ca^{2+} response

Increases in the cytosolic [Ca^{2+}] in response to threshold concentrations of UTP (30–300 nM) were assessed in single Lvec (**A**) and L15 (**B**) fura-2-loaded (2 μM, 60 min) cells. UTP was added to cells by continuous perfusion, followed by a wash-out step with KHB. Traces show single Lvec and L15 cells representative of three to five separate experiments (number of Lvec and L15 cells examined: 30 nM UTP, $n = 17$, 18; 100 nM, $n = 34$, 22; 300 nM, 37, 24 respectively).

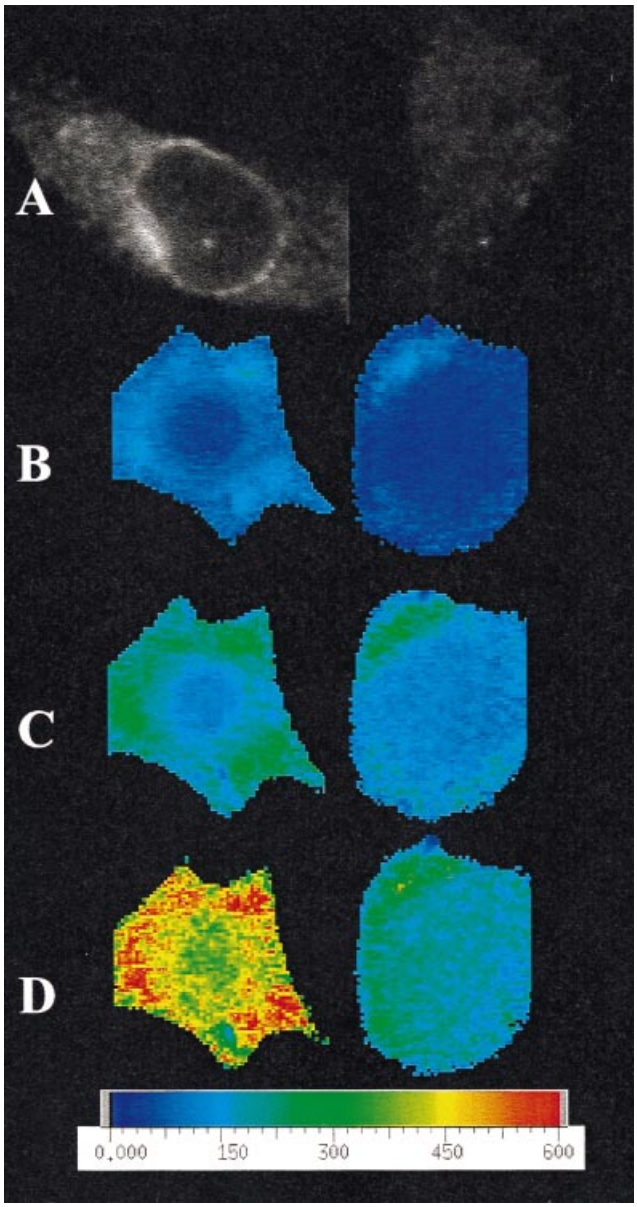

Figure 4 Localization of type 1 InsP_3R expression and basal and agonist-stimulated changes in $[Ca^{2+}]_i$ in L15 and Lvec cells

(**A**) Shows the expression of type 1 InsP_3R in L15 (left) and Lvec (right) cells revealed by immunostaining with the InsP_3R1 CT-1 antibody and FITC-conjugated anti-rabbit IgG, and revealed using confocal microscopy (representative example from three separate experiments, each involving multiple Lvec and L15 samples treated with different dilutions of primary/secondary antibodies). (**B**)–(**D**) Show representative pseudo-colour images of cytosolic [Ca^{2+}] in L15 (left) and Lvec (right) cells. Images were taken under basal conditions (**B**) and 1.6 s (**C**) and 3.2 s (**D**) following addition of 3 μM UTP. Magnification was $\times$ 455 for (**A**) and $\times$ 365 for (**B**)–(**D**) (see the Materials and methods section for further details).

responses to agonist were substantially greater in the L15 cells (Figure 1), while UTP and ATP were equipotent in the two cell lines [e.g., for UTP, $-\log EC_{50}$ (M): Lvec, 5.36 ± 0.04 (4.7 μM); L15, 5.18 ± 0.12 (6.6 μM); see Figure 1C]. The effects of UTP and ATP on cytosolic [Ca^{2+}] were non-additive, suggesting that both agonists work through the same receptor/signalling cascade. Both ATP and UTP were substantially more potent than 2-methylthio-ATP (2MeS-ATP), for which increases in cytosolic [Ca^{2+}] were only observed at concentrations of $\geqslant 100$ μM (results not shown). An agonist potency ranking of ATP = UTP $\gg$ 2MeS-ATP is consistent with an endogenous $P2Y_2$ purinoceptor in L-fibroblast cells, in agreement with conclusions reached previously by others [20].

Agonist-mediated peak increases in cytosolic [Ca^{2+}] resulted primarily from a mobilization of Ca^{2+} from intracellular stores. Thus UTP-stimulated increases in the peak cytosolic [Ca^{2+}] response were not significantly different under nominally Ca^{2+}-free conditions compared with the presence of millimolar extracellular Ca^{2+}. In contrast, in the absence of extracellular Ca^{2+}, $[Ca^{2+}]_i$ profiles completely lacked a plateau phase, which could be recovered on re-addition of 2 mM Ca^{2+}. Ca^{2+} re-addition resulted in comparable increases in the cytosolic [Ca^{2+}] in each cell line (results not shown).

Pre-treatment of Lvec and L15 cells with pertussis toxin (PTX; 100 ng/ml for 20–24 h) to inhibit G_i-coupled signalling, did not modify cytosolic [Ca^{2+}] profiles in response to the addition of UTP, at either submaximal (5 μM) or maximal (300 μM) concentrations, in either the absence or presence of extracellular

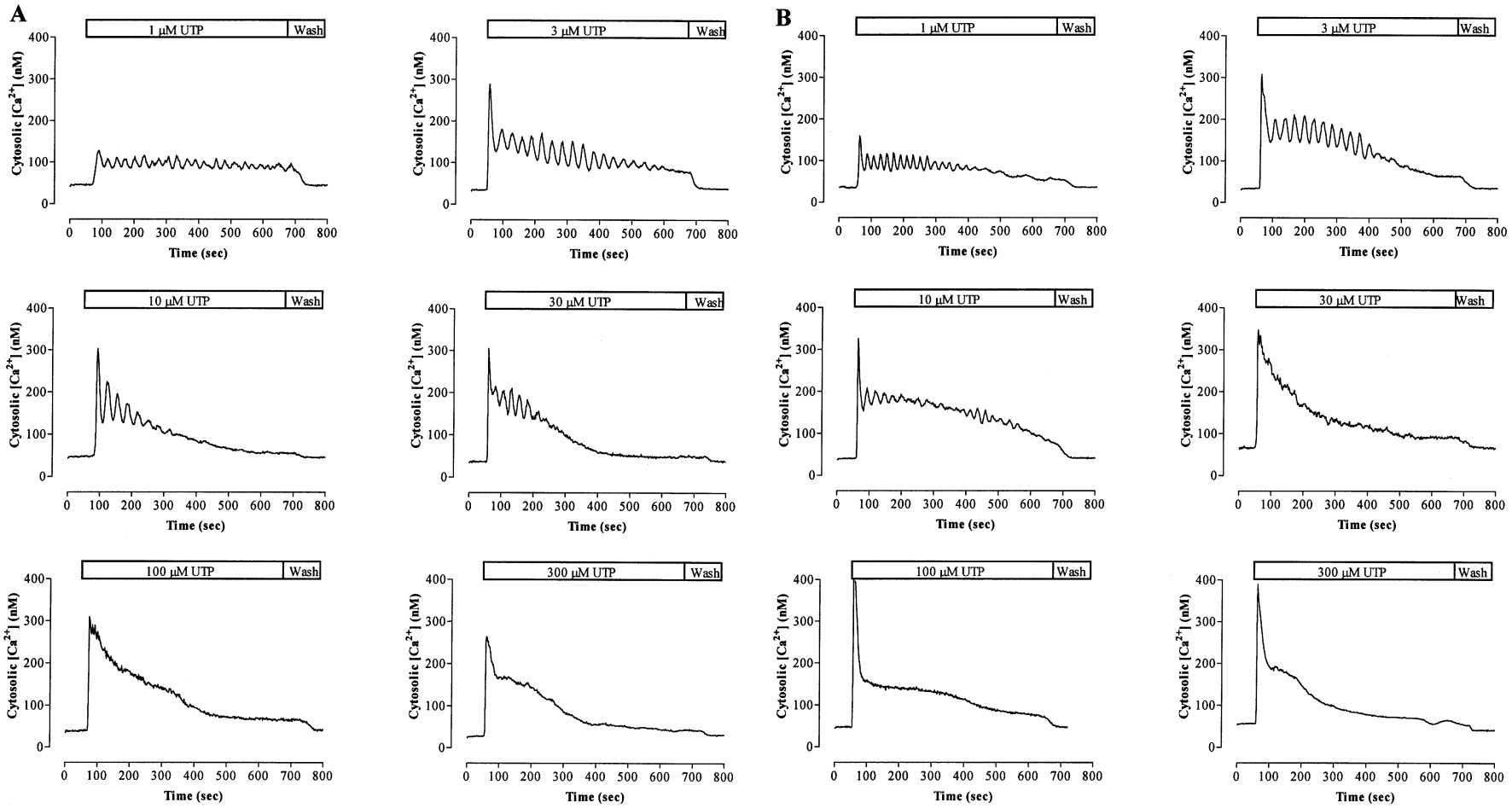

Figure 5 Complex cytosolic [Ca^{2+}] responses stimulated by purinoceptor activation in single Lvec and L15 cells

Fura-2-loaded Lvec (**A**) and L15 (**B**) cells produced cytosolic Ca^{2+} oscillations in response to continual perfusion with submaximal concentrations of UTP. At higher UTP concentrations, oscillatory responses were superseded by biphasic peak-and-plateau responses. Traces show representative single-cell responses from three to five separate experiments (number of Lvec and L15 cells; 1 μM, $n = 21, 36$; 3 μM, $n = 31, 47$; 10 μM, $n = 24, 64$; 30 μM, $n = 16, 33$; 100 μM, $n = 35, 26$; 300 μM, $n = 21, 38$ respectively).

Ca^{2+} (results not shown). These data strongly implicate $G_{q/11}$-activated phospholipase C-β and $Ins P_3$-mediated Ca^{2+} signalling.

In the presence of extracellular Ca^{2+}, treatment of Lvec- and L15-cell populations with thapsigargin (Tg) (1 μM), to inhibit irreversibly sarco-/endo-plasmic-reticular Ca^{2+}-ATPase (SERCA) pumps and cause depletion of the intracellular Ca^{2+} store, resulted in a rapid (< 20 s), sustained increase in cytosolic [Ca^{2+}] (basal, 55 ± 3 and 68 ± 6; +Tg, 203 ± 4 and 207 ± 3 nM in Lvec and L15 cells respectively). In the absence of extracellular Ca^{2+} this increase was transient and smaller (basal, 46 ± 7 and 45 ± 5; +Tg (peak), 140 ± 6 and 139 ± 4 nM in Lvec and L15 cells respectively). In each case pretreatment with 1 μM Tg for 10 min abolished the purinoceptor-mediated response. These experiments strongly suggest that these cell lines possess identical Tg-sensitive Ca^{2+} stores.

Purinoceptor activation stimulates the accumulation of $Ins P_3$ in Lvec and L15 cells

Similar time-courses of $Ins P_3$ mass accumulation were seen in L15 and Lvec cell lines in response to maximally effective concentrations (300 μM) of UTP or ATP. Agonist-stimulated $Ins P_3$ accumulations were characterized by an increase to peak within 30 s, followed by a gradual return to near basal levels within 5 min (Figure 2A). Basal $Ins P_3$ levels in the Lvec and L15 cells were similar (Lvec, 28 ± 1; L15, 30 ± 3 pmol/mg of protein, $n = 4$), and increased on stimulation to similar peak values (Lvec, 65 ± 3; L15, 70 ± 5 pmol/mg of protein, $n = 4$). Stimulation of Lvec and L15 cells with increasing concentrations of UTP or ATP (10–1000 μM) produced similar concentration-dependent elevations in $Ins P_3$ [$-\log EC_{50}$ (M) values: Lvec, 4.20 ± 0.26 (63 μM); L15, 4.23 ± 0.25 (60 μM); see Figure 2B].

Ca^{2+} signalling in single cells: overexpression of the type 1 $Ins P_3$R reduces the threshold for agonist action

To examine the threshold for agonist-mediated Ca^{2+} signalling in single fura-2-loaded Lvec and L15 cells, low-nanomolar concentrations of UTP were added by perfusion in the presence of extracellular Ca^{2+} (Figures 3A and 3B). Neither cell line responded to the application of 30 nM UTP ($n = 17/18$ for Lvec/L15 cells, three independent experiments). However, in comparison with Lvec, L15 cells consistently responded to a lower threshold application of UTP. Thus 100 nM UTP increased cytosolic [Ca^{2+}] by approx. 70–100 nM in L15 cells ($n = 34/22$ for Lvec/L15 cells, three independent experiments), whereas Lvec cells failed to respond until the UTP concentration was increased to 300 nM ($n = 37/24$ for Lvec/L15 cells, three independent experiments). The reproducibility of the threshold differential for UTP stimulation provides confirmation that individual Lvec and L15 cells are representative of each homogenous cell population and that all L15 cells overexpress $Ins P_3$Rs. At 300 nM UTP, L15 cells consistently exhibited complex sinusoidal patterns of cytosolic Ca^{2+} oscillation (see Figure 3B).

Ca^{2+} signals initiate from localized regions of the cytoplasm

Ca^{2+} signals appeared to initiate from specific 'hot-spot' areas within the cytoplasm (Figures 4B–4D) and were more apparent in L15 cells. These areas had higher basal [Ca^{2+}] and showed the most rapid increases in [Ca^{2+}] on agonist challenge. To show that these 'hot-spot' areas were not 'artifactually' caused by fura-2 sequestration into organellar structures, saponin (10 μg/ml) was added to permeabilize selectively the plasma membrane (of L15 cells). This led to an immediate and total loss of all fura-2 from all areas of the cell (measured by excitation at the 360 nm excitation isosbestic point; $n = 34$; results not shown). Furthermore, we could find no evidence for Mn^{2+}-quench occurring more rapidly close to 'hot-spots'; rather, decreases in fluorescence seemed to occur uniformly across L15 cells ($n = 12$ from four independent experiments; results not shown).

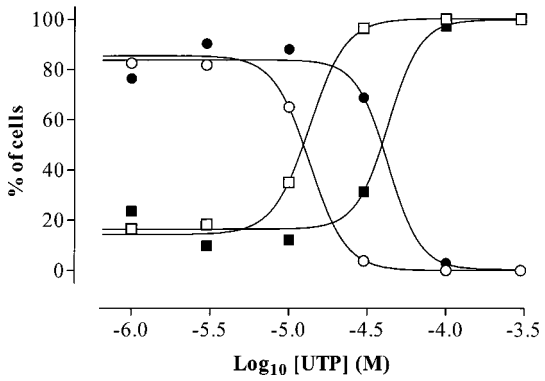

Figure 6 Effects of $Ins P_3$R overexpression on the concentration-dependent changes in temporal patterns of Ca^{2+} signalling mediated by UTP

Analysis of the percentage of cells producing either oscillatory or peak-and-plateau cytosolic Ca^{2+} responses with increasing agonist concentration demonstrated that L15 cells (oscillatory, ○; peak and plateau, □) exhibit a lower threshold for the transformation of oscillatory responses into biphasic peak-and-plateau responses relative to Lvec cells (●, oscillatory; ■, peak and plateau). Data are expressed as mean values for the percentage of all cells exhibiting an oscillatory or peak-and-plateau response at each UTP concentration (see Figure 5 for sample sizes and the text for EC_{50} values).

Lvec and L15 cells produce complex, temporally organized cytosolic Ca^{2+} responses at low agonist concentrations

Continual application (for approx. 10 min) of submaximal concentrations of UTP to Lvec and L15 cell lines produced sinusoidal Ca^{2+} oscillations superimposed on a raised basal [Ca^{2+}] (see Figures 5A and 5B). Removal of UTP caused an immediate cessation in oscillatory or plateau cytosolic [Ca^{2+}] and a return to prestimulation levels. The data from Figure 5 reveal that there is a constant frequency of oscillations at different agonist concentrations in both cell lines, although there was a significantly greater frequency in agonist-stimulated L15 than in Lvec cells {e.g. trough-to-trough time (s): Lvec, 19.1 ± 0.2; L15, 22.1 ± 0.6 ($n = 49$; $P < 0.01$) at 3 μM UTP in the presence of normal $[Ca^{2+}]_e$}. At higher agonist concentrations, oscillatory Ca^{2+} responses were superseded by biphasic peak-and-plateau responses. The threshold for the transition between oscillatory and peak-and-plateau responses was significantly different between cell lines, with the transition occurring at lower UTP concentrations in L15 compared with Lvec cells [$-\log EC_{50}$ (M) values: Lvec, 4.41 ± 0.19 (39 μM); L15, 4.91 ± 0.05 (12 μM) ($P < 0.05$); see Figure 6].

DISCUSSION

In the present study we have utilized mouse L-fibroblast cells transfected with either type 1 $Ins P_3$R cDNA (L15) or the empty vector (Lvec) to investigate the functional consequences of $Ins P_3$R density on cell-surface receptor-mediated $Ins P_3$-induced Ca^{2+} signalling. Previously we have reported on the stability of the $Ins P_3$R overexpression and the subcellular distribution of the recombinant $Ins P_3$Rs in this clonal cell line [19]. L15 cells stably overexpress approx. 8-fold the levels of $Ins P_3$R1 compared with

Lvec cells, which in turn endogenously express essentially only the type 1 InsP_3R protein [19]. Here we have confirmed the overexpression of InsP_3R protein in L15 cells using immunocytochemistry [18] and demonstrated an unequal distribution of (recombinant) InsP_3Rs with prominent antibody staining in the perinuclear region. It should be noted that our studies represent, to the best of our knowledge, the only report of a stable overexpression of InsP_3R with an appropriate subcellular distribution in a mammalian cell line. Overexpression of the type 3 InsP_3R in βTC-3 insulinoma cells has been reported to be particularly unstable, declining with passage [23]. Likewise, in NIH-3T3 fibroblasts transfected with full-length or truncated type 1 InsP_3R, cDNA expression levels of only $15-30\%$ above that of the endogenous receptor were achieved, owing to a change in the turnover of InsP_3R proteins following transfection [24], and other complex adaptative changes (e.g. a reduction in receptor-mediated InsP_3 production) occurred following transfection [24]. However, more recently overexpression of the types 1 and 3 InsP_3Rs has been achieved in *Xenopus* oocytes [25] and *Spodoptera frugiperda* (Sf9) insect cells [10,26]. In the former study, InsP_3R1 overexpression in oocytes was shown to enhance cytosolic Ca^{2+} wave propagation, presumably via an increased rate of intracellular Ca^{2+} release, whereas type 3 InsP_3R overexpression enhanced Ca^{2+} entry [25].

The present study confirms that L-cells endogenously express metabotropic purinoceptors coupled to phosphoinositide hydrolysis [20], and this has provided us with a model system in which to investigate the potential consequences of InsP_3R overexpression on agonist-mediated signalling. The purine ATP and pyrimidine UTP were found to be equipotent agonists in both Lvec and L15 cells with respect to InsP_3-generation and Ca^{2+}-mobilization responses, whereas the synthetic analogue 2-methylthio-ATP was much less potent. These data strongly suggest the presence of G-protein-coupled metabotropic P2Y purinoceptor, probably of the $P2Y_2$ subtype, in L-fibroblasts [27]. Furthermore, in both L-cell clones, agonist-mediated InsP_3 generation was unaffected by changes in InsP_3R expression, suggesting that transfection/overexpression has little influence on upstream components of the purinoceptor-mediated signalling cascade in these cells. This contrasts with a previous study in NIH-3T3 cells in which compensatory reductions in the level of InsP_3 production by down-regulation of endogenous P_{2U} ($P2Y_2$) purinoceptors followed the overexpression of truncated InsP_3R mutants [24].

Downstream of InsP_3 generation, Ca^{2+} signalling was significantly enhanced in populations of L15 cells at all levels of purinoceptor stimulation. The enhancement in the peak Ca^{2+} signal was due to increased Ca^{2+} mobilization, as opposed to increased Ca^{2+} entry, as the enhancement was still observed in experiments performed in the absence of extracellular Ca^{2+}. This enhanced response would be consistent with the greater capacity of the increased number of InsP_3Rs to release Ca^{2+} and would be supported by our previous studies on the subcellular distribution of endogenous and transfected InsP_3R1 in L-cells [19]. In those experiments, expression of InsP_3R1 occurred within compartments bearing SERCA pumps and crucially was associated with an increased sensitivity of Ca^{2+} mobilization to InsP_3 and several metabolically stable inositol (poly)phosphate analogues in permeabilized L15 cells [19,28]. It should also be noted that we demonstrate here that Lvec and L15 cells possess similar intracellular Ca^{2+} stores, using Tg to assess pool size.

Following stimulation of single cells with threshold and submaximal agonist concentrations cytosolic Ca^{2+} was shown to be released in an oscillatory fashion. Fluctuations in cytosolic Ca^{2+} signalling in the form of oscillations or 'spiking' have been observed in a wide variety of cell when receptors activating the phosphoinositide signalling cascade are stimulated. There are a variety of oscillatory patterns which are determined by such factors as cell specificity, agonist type and concentration, as well as extracellular Ca^{2+} concentration (see [29,30]). In L-cells, the pattern of oscillations can be categorized as being sinusoidal, as opposed to baseline spiking, because oscillations occur over and above an elevated plateau Ca^{2+} level [31]. Such sinusoidal oscillations can be explained by a simple negative feedback and, in the case of lacrimal acinar cells activated by muscarinic receptors, such feedback is mediated by protein kinase C acting on, or proximal to, phospholipase C [32]. This model proposes oscillating phospholipase C activity with $[Ca^{2+}]_i$ simply reflecting InsP_3 and diacylglycerol fluctuations [31]. Preliminary data would support such a mechanism in L-cells in that pharmacological inhibition or down-regulation of protein kinase C abolishes UTP-mediated oscillations in both Lvec and L15 cells (R. J. Davis, R. A. J. Challiss and S. R. Nahorski, unpublished work).

Direct comparison of Lvec and L15 cells revealed clear differences in single-cell Ca^{2+}-signalling patterns. L15 cells produce cytosolic Ca^{2+} responses to lower threshold concentrations of UTP compared with Lvec cells, and the transition from oscillatory to peak-and-plateau responses also occurred at lower agonist concentrations in cells overexpressing InsP_3Rs. These differences cannot be attributed to changes in any upstream component of the purinoceptor signalling cascade, changes in the InsP_3R isoform or alterations in InsP_3 binding affinity for its receptor [19]. The current data suggest that they directly reflect the functional overexpression of InsP_3Rs in L15 cells, which would be expected to reduce the threshold for InsP_3, both to initiate Ca^{2+} oscillations and to transform them into a sustained increase in $[Ca^{2+}]_i$. Whether this relates simply to a greater density of InsP_3Rs, or to interactions between 'stacked' channels, or to an altered stoichiometry with other modulators, remains to be established.

Finally, in the present study, agonist-stimulated Ca^{2+} signals appeared to initiate from localized regions of the cytoplasm. These 'hot-spots' were greater in both resting and stimulated L15 cells, though one should be cautious in directly correlating these initiation regions with the immunocytochemical localization of type 1 InsP_3Rs in L cells. These areas are of course far too large, and the time-scale too slow, to be accounted for by the opening of single or even small clusters of discrete InsP_3Rs. They may arise in regions of high InsP_3R density because of increased unstimulated passive Ca^{2+} leak through InsP_3R channels. Assuming that there are multiple stores, perhaps associated with compartmentation of the endoplasmic reticulum, heterogeneity of InsP_3R density coupled to differing resting $[Ca^{2+}]$ in 'hot-spots' could be expected to initiate global Ca^{2+} signals from such regions. Clarification on these important issues obviously requires imaging of cellular Ca^{2+} at a much greater resolution. These studies have been initiated using a Ca^{2+}-imaging/confocal-microscopy approach.

Our data are strongly consistent with a model in which increased InsP_3R expression in L15 cells results in an enhanced maximal Ca^{2+} signal as seen in the population studies, a corresponding reduced threshold concentration of agonist to initiate oscillations and an increased frequency of oscillations at a particular agonist concentration, in single L15 cells. Overall, the present experiments demonstrate how stable overexpression of type 1 InsP_3Rs in L-cells significantly enhances purinoceptor-mediated Ca^{2+} signalling. InsP_3R density would therefore seem to be an important determinant of temporal Ca^{2+} signalling for a given cell type. In addition, the ability of cells to regulate the expression of different isoforms of InsP_3R either during de-

velopment [33–35], differentiation [36] or persistent agonist activation [13,14] may represent an important regulatory feature of receptor-mediated Ca^{2+} signalling.

This work was supported by a Programme Grant (reference no. 016895/96) from the Wellcome Trust of Great Britain. R.J.D. held a Biotechnology and Biological Sciences Research Council of Great Britain Research Studentship. We thank Professor K. Mikoshiba for initially providing us with the Lvec and L15 cell lines. We also thank Dr. K. W. Young for his expertise and assistance in single-cell Ca^{2+}-imaging experiments, Mr. R. Mistry for performing the InsP_3 mass measurements, and Dr. G. B. Willars for statistical expertise and critical reading of earlier drafts of the manuscript.

REFERENCES

1 Berridge, M. J. (1993) Nature (London) **361**, 315–325
2 Furuichi, T., Yoshikawa, S., Miyawaki, A., Wada, K., Maeda, N. and Mikoshiba, K. (1989) Nature (London) **342**, 32–38
3 Südhof, T. C., Newton, C. L., Archer, B. T., Ushkaryov, Y. A. and Mignery, G. A. (1991) EMBO J. **10**, 3199–3206
4 Ross, C. A., Danoff, S. K., Schell, M. J., Synder, S. H. and Ullrich, A. (1992) Proc. Natl. Acad. Sci. U.S.A. **89**, 4256–4269
5 Blondel, O., Takeda, J., Janssen, H., Seino, S. and Bell, G. I. (1993) J. Biol. Chem. **268**, 11356–11363
6 Bezprozvanny, I, Watras, J. and Ehrlich, B. E. (1991) Nature (London) **351**, 751–754
7 Newton, C. L., Mignery, G. A. and Südhof, T. C. (1994) J. Biol. Chem. **269**, 28613–28619
8 Wojcikiewicz, R. J. H. (1995) J. Biol. Chem. **270**, 11678–11683
9 Jayaraman, T., Ondrias, K, Ondriasova, E. and Marks, A. R. (1996) Science **272**, 1492–1494
10 Yoneshima, H., Miyawaki, A., Michikawa, T., Furuichi, T. and Mikoshiba, K. (1997) Biochem. J. **322**, 591–596
11 Mikoshiba, K. (1997) Curr. Opin. Neurobiol. **7**, 339–345
12 Wojcikiewicz, R. J. H. and Luo, S. G. (1998) J. Biol. Chem. **273**, 5670–5677
13 Wojcikiewicz, R. J. H., Furuichi, T., Nakade, S., Mikoshiba, K. and Nahorski, S. R. (1994) J. Biol. Chem. **269**, 7963–7969
14 Sharma, K., Wang, L., Zhu, Y., Bokkala, S. and Joseph, S. K. (1997) J. Biol. Chem. **272**, 14617–14623
15 Sipma, H., Deelman, L., De Smedt, H., Missiaen, L., Parys, J. B., Vanlingen, S., Henning, R. H. and Casteels, R. (1998) Cell Calcium **23**, 11–21
16 Bradford, P. G., Wang, X., Jin, Y. and Hui, P. (1992) J. Biol. Chem. **267**, 20959–209640
17 Khan, A. A., Soloski, M. J., Sharp, A. H., Schilling, G., Sabatini, D. M., Li, S.-H., Ross, C. A. and Snyder, S. H. (1996) Science **273**, 503–507
18 Miyawaki, A., Furuichi, T, Maeda, N. and Mikoshiba, K. (1990) Neuron **5**, 11–18
19 Mackrill, J.J, Wilcox, R. A., Miyawaki, A., Mikoshiba, K., Nahorski, S. R. and Challiss, R. A. J. (1996) Biochem. J. **318**, 871–878
20 Grierson, J. P. and Meldolesi, J. (1995) J. Biol. Chem. **270**, 4451–4456
21 Challiss, R. A.J, Chilvers, E. R., Willcocks, A. L. and Nahorski, S. R. (1990) Biochem. J. **265**, 421–427
22 Grynkiewicz, G., Poenie, M. and Tsien, R. Y. (1985) J. Biol. Chem. **260**, 3440–3450
23 Blondel, O., Bell, G. I., Moody, M., Miller, R. J. and Gibbons, S. J. (1994) J. Biol. Chem. **269**, 27167–27170
24 Fischer, G. A., Clementi, E., Raichman, M., Südhof, T., Ullrich, A. and Meldolesi, J. (1994) J. Biol. Chem. **269**, 19216–19224
25 Delisle, S., Blondel, O., Longo, F. J., Schnabel, W. E., Bell, G. I. and Welsh, M. J. (1996) Am. J. Physiol. **270**, C1255–C1261
26 Cardy, T. J. A., Traynor, D. and Taylor, C. W. (1997) Biochem. J. **328**, 785–793
27 Lustig, K. D., Shiau, A. K., Brake, A. J. and Julius, D. (1993) Proc. Natl. Acad. Sci. U.S.A. **90**, 5113–5117
28 Davis, R.J, Wilcox, R. A., Challiss, R. A. J. and Nahorski, S. R. (1997) Abstr. Am. Chem. Soc. **214**(1), p31-CARB
29 Berridge, M. J. (1991) Cell Calcium **12**, 63–72
30 Berridge, M. J. (1997) J. Physiol. (London) **499**, 291–306
31 Thomas, A. P., Bird, G. S. J., Hajnoczky, G., Robb-Gaspars, L. D. and Putney, J. W. (1996) FASEB J. **10**, 1505–1517
32 Bird, G. S. J., Rossier, M. F., Obie, J. F. and Putney, J. W. (1993) J. Biol. Chem. **268**, 8425–8428
33 Venkatesh, K. and Hasan, G. (1997) Curr. Biol. **7**, 500–509
34 Acharya, J. K., Janlink, K., Hardy, R. W., Hartenstein, V. and Zucker, C. S. (1998) Neuron **18**, 881–887
35 Matsumoto, M., Nakagawa, T., Inoue, T., Nagata, E., Tanaka, K., Takano, H., Minowa, O., Kuno, J., Sakakibara, S., Yamada, M. et al. (1996) Nature (London) **379**, 168–171
36 Igwe, O. J. and Filla, M. B. (1995) Neuroscience **69**, 1239–1251

Received 23 February 1999/21 April 1999; accepted 4 June 1999